

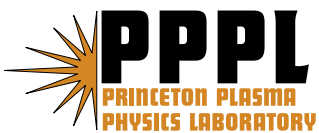
PPPL-4129

PPPL-4129

**A Marker Method for the Solution
of the Damped Burgers' Equation**

Jerome L.V. Lewandowski

November 2005



Princeton Plasma Physics Laboratory

Report Disclaimers

Full Legal Disclaimer

This report was prepared as an account of work sponsored by an agency of the United States Government. Neither the United States Government nor any agency thereof, nor any of their employees, nor any of their contractors, subcontractors or their employees, makes any warranty, express or implied, or assumes any legal liability or responsibility for the accuracy, completeness, or any third party's use or the results of such use of any information, apparatus, product, or process disclosed, or represents that its use would not infringe privately owned rights. Reference herein to any specific commercial product, process, or service by trade name, trademark, manufacturer, or otherwise, does not necessarily constitute or imply its endorsement, recommendation, or favoring by the United States Government or any agency thereof or its contractors or subcontractors. The views and opinions of authors expressed herein do not necessarily state or reflect those of the United States Government or any agency thereof.

Trademark Disclaimer

Reference herein to any specific commercial product, process, or service by trade name, trademark, manufacturer, or otherwise, does not necessarily constitute or imply its endorsement, recommendation, or favoring by the United States Government or any agency thereof or its contractors or subcontractors.

PPPL Report Availability

Princeton Plasma Physics Laboratory

This report is posted on the U.S. Department of Energy's Princeton Plasma Physics Laboratory Publications and Reports web site in Fiscal Year 2006.

The home page for PPPL Reports and Publications is:

http://www.pppl.gov/pub_report/

Office of Scientific and Technical Information (OSTI):

Available electronically at: <http://www.osti.gov/bridge>.

Available for a processing fee to U.S. Department of Energy and its contractors, in paper from:

U.S. Department of Energy
Office of Scientific and Technical Information
P.O. Box 62
Oak Ridge, TN 37831-0062

Telephone: (865) 576-8401

Fax: (865) 576-5728

E-mail: reports@adonis.osti.gov

A marker method for the solution of the damped Burgers' Equation

Jerome L. V. Lewandowski
Princeton University
Plasma Physics Laboratory,
Princeton, NJ 08543, USA

October 20, 2005

Abstract

A new method for the solution of the damped Burgers' equation is described. The marker method relies on the definition of a convective field associated with the underlying partial differential equation; the information about the approximate solution is associated with the response of an ensemble of markers to this convective field. Some key aspects of the method, such as the selection of the shape function and the initial loading, are discussed in some details. The marker method is applicable to a general class of nonlinear dispersive partial differential equations.

1 Introduction

Marker methods have been used for a long time in various disciplines (e.g plasma physics, astrophysics, etc.) to give numerical solution of purely convective problems [7, 8]. Marker methods, sometime called particle methods, have been successfully applied to various physical problems such as the dynamics of galaxies [1], the properties of ionic microcrystals [2], the anomalous diffusion [3] and the resonant effects in Langmuir modes [5] in plasmas and the electron flow in semiconductors [4]. The interested reader can consult the review paper of Dawson [6] and references therein.

In these methods an ensemble of markers (or 'superparticles') is used to approximate the solution; the region of interest covered by the markers defines the phase space associated with the solution. Each marker is represented through its weight and position in phase space. The markers are advanced in time according to the characteristics ('equations of motion') of the underlying partial differential equation (PDE) associated with the problem. Marker methods are particularly useful for collisionless problems [7–9, 12]. However, in many applications of interest (e.g turbulent plasmas), diffusive processes can be important. Marker methods usually include diffusive effects in a perturbative fashion [10, 11]: in the first step, the markers are evolved in phase space according to the collisionless (*i.e.* purely convective) dynamics; in the second step, diffusive effects are included by a randomization of the markers' weights and/or positions according to a prescribed probability distribution. Although this method agrees with physical intuition, it is, from the numerical point of view, quite noisy and possibly inaccurate. The marker method presented in this paper allows for the *simultaneous* treatment of convective and diffusive effects.

The main idea behind the marker method for the solution of a given PDE is to rewrite it as a conservation equation with a generalized convective velocity. In general (even in linear cases), the generalized convective velocity depends on the solution of the PDE itself. Each marker, which carries the information of the solution of the PDE through its weight and its position, is advanced in time using a Lagrangian scheme. The generalized convective velocity mentioned earlier is computed through the information contained in the ensemble of markers and through the so-called shape function.

As it will become apparent in the next sections, the marker method can actually be applied to solve a more general class of PDEs that are encountered commonly in physical and engineering sciences.

The marker method, unlike the finite difference and the finite element methods, does not rely on the concept of a grid (of course one can, if needed, reconstruct the solution on a fixed grid through the collective information associated with the markers). Increased resolution can be achieved in a natural way by locally increasing the number of markers and/or modifying the initial loading of the markers. Unlike the finite difference method, the marker method can be trivially extended to multi-dimensional problems.

This paper is organized as follows; in section 2, the marker method is described in the context of the solution of a one-dimensional linear diffusion equation. The shape function, which is involved in the evaluation of the approximate solution, is analyzed in some detail and a numerical example is presented. The marker method is applied to the nonlinear (undamped) Burgers' equation [14] in section 3. The damped Burgers's equation is discussed in section 4. Concluding remarks are given in section 5.

2 Marker Method

The purpose of this paper is to present a new numerical method for the solution of the nonlinear damped Burgers' equation given by

$$\frac{\partial f}{\partial t} + f \frac{\partial f}{\partial x} = -\nu f + \mu \frac{\partial^2 f}{\partial x^2} , \quad (1)$$

with initial conditions $f(x, 0) = f_0(x)$ and μ and ν are positive constants. However since exact solutions to the standard form of Burgers' equation [14]

$$\frac{\partial f}{\partial t} + f \frac{\partial f}{\partial x} = \mu \frac{\partial^2 f}{\partial x^2} , \quad (2)$$

are known, we have found instructive to consider a numerical study of this equation first.

As mentioned in the Introduction, particle methods are usually applied to purely convective problems [*i.e.* by neglecting the right-hand side in Eq.(1)]. Therefore, the new aspect of the marker method is best described in the context of a simple example: the linear diffusion equation which is a limiting case of Eq.(1). An analysis of the smoothing approximation obtained through the shape function, which represents a crucial aspect of the method, is also discussed in this section. A specific numerical application of the marker method to the case of a one-dimensional linear diffusion equation is given.

2.1 Basic Idea

For illustrative purposes, we describe the marker method for one-dimensional problems (as mentioned in the Introduction, the generalization to multi-dimensional problems is

straightforward). We consider an ensemble of N markers. Each marker k is defined through its position x_k and its weight W_k . The solution of a given one-dimensional PDE is found by allowing the set $\{(x_k, W_k); k = 1, \dots, N\}$ to evolve in time according to a generalized nonlinear convective velocity. The generalized convective velocity usually depends on the solution itself and a form of convolution of the approximate solution with a shape function is required.

Consider the one-dimensional diffusion equation

$$\frac{\partial f}{\partial t} = \frac{\partial^2 f}{\partial x^2} , \quad (3)$$

subject to the initial condition $f_0(x) = f(x, 0)$. The main idea behind the marker method is to write Eq.(3) as a (nonlinear) conservation equation

$$\frac{\partial f}{\partial t} + \frac{\partial}{\partial x} (Vf) = 0 , \quad (4)$$

where

$$V = -\frac{1}{f} \frac{\partial f}{\partial x} . \quad (5)$$

For clarity, $f(x, t)$ is used to denote the exact solution of Eq.(3) whereas $F(x, t)$ represents its approximation. The function f can be approximated by an ensemble of markers (or ‘superparticles’) where each marker j has an associated weight, W_j , and a time-dependent position, $x_j(t)$. As in standard particle methods, such an approximation can be written in terms of delta functions [7, 8]

$$\widehat{F} = \sum_{j=1}^N W_j \delta(x - x_j) , \quad (6)$$

where $\delta(x)$ is the usual Kronecker delta function; the hat notation indicates that the representation is singular. For example, $1/\widehat{F}(x, t)$ can be singular in region where $f(x, t)$ is nonzero; furthermore, the ratio of delta functions is not defined. Substituting the discrete representation (6) in Eq.(4) yields the characteristics associated with the generalized velocity V

$$\left. \begin{aligned} dx_j/dt &= V(x_j(t), t) \\ x_j(0) &= x_{0j} \end{aligned} \right\} j = 1, \dots, N \quad (7)$$

As noted above, $V \propto \partial \widehat{F} / \partial x / \widehat{F}$ is not well defined. As in conventional particle methods, a smoothed version of \widehat{F} is obtained by taking the convolution of Eq.(6) with a shape function

$$F(x, t) = (S_\epsilon \star \widehat{F})(x, t) = \sum_{j=1}^N W_j S_\epsilon(x - x_j) , \quad (8)$$

where $S_\epsilon(x) = S(x/\epsilon)/\epsilon$ and $\int S dx = 1$; ϵ is termed the support parameter. Using representation (8) in the trajectory equations, Eq.(7), one gets

$$\frac{dx_j}{dt} = -\frac{\sum_{k=1}^N W_k S'_\epsilon(x_j(t) - x_k(t))}{\sum_{k=1}^N W_k S_\epsilon(x_j(t) - x_k(t))} \quad (9)$$

where a prime denotes a derivative with respect to the argument and the initial positions are $x_j(0) = x_{0j}$. Note that the weights in Eq.(9) do not vary in time; in particular, if all the weights are initially equal, then all the information about the approximation $F(x, t)$ is contained in the marker positions. The equations of motion (9) can be integrated using standard ordinary differential equation (ODE) techniques, such as the Runge-Kutta method [18], as used in this paper.

Before considering a numerical illustration of the marker method, several observations are in order. Clearly the accuracy of the marker method depends crucially on the shape function and its support parameter, ϵ (see next section). The number of markers, the method of integration of the equations of motion, the initial loading of the ensemble $\{(x_k, W_k); k = 1, \dots, N\}$ and the time step of integration are parameters that also influence the accuracy of the marker method. In some sense, the positions of the markers define a moving grid as far as the approximate solution is concerned. Of course one can reconstruct the approximate solution F on a fixed grid $\{X_g; g = 1, \dots, N_g\}$ at time t by invoking the representation (8):

$$F_g(t) = F(X_g, t) = \sum_{j=1}^N W_j S_\epsilon(X_g - x_j(t)) .$$

The marker method can be easily generalized to *nonlinear* dispersive PDEs such as the Korteweg de Vries (KdV) equation [13] and Burgers' equation. For example, the KdV equation [13]

$$\frac{\partial f}{\partial t} + 3\frac{\partial f^2}{\partial x} + \frac{\partial^3 f}{\partial x^3} = 0 ,$$

can be written as a nonlinear conservation equation [Eq.(4)] with a generalized velocity

$$V(x, t) = 3f(x, t) + \frac{\partial^2 f(x, t)/\partial x^2}{f(x, t)} ,$$

as it can be verified by direct substitution. Therefore the marker method is very versatile in its applications, whereas conventional (*e.g.* finite difference) methods usually require substantial modifications to account for additional nonlinear or dispersive terms, for example. This is illustrated in section 3 where the marker method is shown to be easily generalized to the case of the nonlinear Burgers' equation.

2.2 Analysis of the Smoothing Approximation and Initial Loading

As mentioned in the previous section, the accuracy of the marker method depends crucially on the properties of the smoothed PDE's approximate solution. Therefore it is important to study the impact of the shape function and its support parameter ϵ on test functions. As it will become apparent below, the accuracy of the smoothing approximation is also related to the initial loading of the markers. The smoothed approximation of the exact solution $f(x)$ is given by

$$F(x) = \sum_{j=1}^N W_j S_\epsilon(x - x_j) \tag{10}$$

where $S_\epsilon(x) = S(x/\epsilon)/\epsilon$ and the shape function $S(x)$ with finite support satisfies the normalization condition

$$\int_{-1}^1 S(x)dx = 1 ,$$

and $S(x) = 0$ for $|x| > 1$. In some cases, there are advantages in using shape functions with infinite support, in which case the normalization condition is of the form $\int_{-\infty}^{+\infty} Sdx = 1$. Apart from the actual form of the shape function, there is some freedom in selecting the value of the support parameter ϵ . However one can estimate an appropriate value for ϵ based on the following considerations. For illustrative purposes, consider a simulation with N markers that are initially distributed uniformly in the interval $x \in [-L, L]$; therefore, at $t = 0$, the average distance between markers is $h = 2L/N$. If the support parameter is such that $\epsilon < h$, then $S_\epsilon(x_j - x_k) \propto S((x_j - x_k)/\epsilon) = 0$ for all markers $j \neq k$; this implies that the position of each marker will be independent of the positions of the other markers at least at $t = 0$. We conclude that the support parameter must be larger than the average distance between markers, at least in the average sense. In addition, the value of ϵ , which is akin to a grid spacing in the finite difference method, must be chosen such as to accurately resolve the spatial scale length of $f(x)$. In summary, if λ denotes the (known or estimated) spatial scale length of $f(x)$ and h is the average distance between markers, the support parameter, ϵ , must satisfy the following inequality

$$h \ll \epsilon \ll \lambda .$$

There is some freedom in selecting a shape function. Typically one requires some smoothness properties and/or ease of computation (for example, a Gaussian shape function is smoother than a hat shape function, but it is computationally more demanding to evaluate). Below is a set of shape functions that are defined on the interval $[-1, +1]$:

$$\begin{aligned} S_1(x) &= \frac{1}{2} \quad (\text{gate function}) \\ S_2(x) &= 1 - |x| \quad (\text{hat function}) \\ S_3(x) &= \frac{3}{4} (1 - x^2) \quad (\text{quadratic polynomial}) \\ S_4(x) &= \frac{15}{16} (1 - x^2)^2 \quad (\text{quartic polynomial}) \\ S_5(x) &= \mu (1 - |x|) e^{-x^2} \quad (\text{hat/Gaussian shape function}) \\ S_6(x) &= \beta (1 - x^2)^2 e^{-x^2} \quad (\text{quartic polynomial/Gaussian shape function}) \end{aligned} \tag{11}$$

where $\mu = (\sqrt{\pi}\text{erf}(1) + 1/e - 1)^{-1}$ and $\beta = 2 / (\frac{3}{2} \text{erf}(1) - 1/e)$ are constants of normalization, and $\text{erf}(x)$ denotes the error function

$$\text{erf}(x) = \frac{2}{\sqrt{\pi}} \int_0^x e^{-t^2} dt .$$

The second factor that affects the approximation of $f(x)$ is the initial distribution of the position of the markers and their associated weights (referred to as the initial loading). There are two basic approaches to the initialization of the ensemble $\{(x_j, W_j) ; j = 1, \dots, N\}$. In the first approach, the markers are uniformly distributed in space. Using the approximation of

$$\int f(x)dx \approx \sum_j f(x_j)\Delta x ,$$

where Δx is the distance between two consecutive markers, and noting that [see Eq.(6)]

$$\int \hat{F} dx = \sum_j W_j ,$$

it follows that

$$\begin{aligned} W_j &= f(x_j)\Delta x \\ x_{j+1} - x_j &= \Delta x = \text{const} . \end{aligned}$$

For the case of a uniform loading we have the relation of $\Delta x = h$. In the second approach, each marker has the same weight, but the spatial distribution of the markers is not uniform. If there are N markers, the marker weight is then $W_j = \sigma/N$ where $\sigma \equiv \int_{-\infty}^{+\infty} f dx$. In order to determine the spatial distribution of the markers, it is convenient to introduce the variable

$$\xi = \frac{\int_{-\infty}^x f(x) dx}{\int_{-\infty}^{+\infty} f(x) dx} ,$$

which, by construction, is a positive-definite quantity in the unit interval. A uniform distribution in ξ , that is $\xi_j = (j - \frac{1}{2})/N$ ($\forall j$), yields

$$\begin{aligned} x_j &= g^{-1} \left(\left(\int_{-\infty}^{+\infty} f(x) dx \right) \frac{j - \frac{1}{2}}{N} \right) \\ W_j &= \frac{\sigma}{N} \end{aligned} \quad (12)$$

where g^{-1} denotes the inverse of $g(x) \equiv \int_{-\infty}^x f(x') dx'$. As a numerical illustration, consider the function

$$f(x) = x e^{-x^2} ,$$

in the interval $x \in [0, x_0]$, $x_0 > 0$. The initialization based on a set of uniformly distributed x_j yields

$$\begin{aligned} x_j &= (j - 1/2)h , \\ W_j &= x_j e^{-x_j^2} h , \end{aligned}$$

where $h = x_0/N$. Alternatively, one can demand that each marker carries an equal weight; following the procedure described above [Eq.(12)] one obtains

$$\begin{aligned} x_j &= \sqrt{-\ln \left(1 - \frac{j - 1/2}{N} (1 - e^{-x_0^2}) \right)} \\ W_j &= \frac{1}{N} , \end{aligned} \quad (13)$$

Fig. 1 shows the smoothed approximation of $f(x)$ for a uniform spatial loading (dotted line) and a nonuniform spatial loading (dashed line) using a quadratic shape function with support parameter $\epsilon = 0.1$ for a set of $N = 32$ markers. The plain line represents the exact function. For the same parameters, the quartic shape function, which satisfies $S'(x = \pm 1) = 0$, yields a better approximation (Fig. 2). Further improvement (Fig. 3) can be achieved using the shape function based on a quartic polynomial and a Gaussian function [$S(x) = S_6(x)$; see Eq.(11)]. Of course, in all the above cases, smoother approximations

can be obtained by increasing the number of markers N . Another parameter affecting the quality of the approximation is the support parameter, ϵ . Fig. 4 is the same as Fig. 2 except that the support parameter has been doubled ($\epsilon = 0.2$). Clearly a much better agreement between the approximated functions and the exact function is found. If the support parameter is further increased the smoothing effect of $S(x)$ becomes too important and the quality of the approximated function degrades.

2.3 Numerical Example for the Linear Diffusion Equation

In this section, we apply the marker method for the diffusion equation, Eq.(3), with initial conditions

$$\left. \begin{aligned} f_0(x) &= 1; |x| \leq 1 \\ &= 0; |x| > 1 \end{aligned} \right\} \quad (14)$$

The solution of the diffusion equation, Eq.(3), with initial conditions (14) is easily found using Laplace transforms

$$\begin{aligned} f(x, t) &= \frac{1}{\sqrt{4\pi t}} \int_{-\infty}^{+\infty} f_0(\xi) \exp(-(x - \xi)^2/4t) d\xi \\ &= \frac{1}{2} \left[\operatorname{erf} \left(\frac{x+1}{2\sqrt{t}} \right) - \operatorname{erf} \left(\frac{x-1}{2\sqrt{t}} \right) \right], \end{aligned}$$

where, as before, $\operatorname{erf}(x)$ is the error function with argument x . As mentioned in the previous section, there is some freedom in the choice of the shape function $S(x)$. Here we consider a shape function with infinite support (superGaussian)

$$S_7(x) = \frac{3/2 - x^2}{\sqrt{\pi}} e^{-x^2}. \quad (15)$$

The equations of motion (9) have been integrated using a second-order Runge-Kutta method with a fixed time step. The approximate solution has been reconstructed on a moving grid defined by the marker positions $\mathbf{x}(t) = \{x_j(t); j = 1, \dots, N\}$. Note that one can determine the approximate solution on a fixed, prescribed grid; however this approach involves the shape function (or some other form of interpolation) that further reduces the accuracy of the numerical scheme. Fig.(5) shows the exact solutions (plain line: $t = 2.0$; dotted line: $t = 4.0$) and the approximate solutions (triangles: $t = 2.0$; squares: $t = 4.0$) of the diffusion equation for a set of $N = 100$ markers. The initial condition is the square profile of Eq.(14). The shape function is a superGaussian [Eq.(15)]; other parameters are $\Delta t = 0.01$, $\epsilon = 1/3$ and $L = 14.0$. We note the excellent agreement of the approximate solution with the exact solutions. As it can be expected, slight errors do appear when $F \mapsto 0$ although their magnitude are small.

Although not shown here, we have noted that the use of a certain shape functions with finite support can sometime lead to a clustering effect in the marker position, that is the solution appears to display an additional scale length associated with the support parameter. In general, the use of shape function with infinite support appear to improve the accuracy of the approximate solution.

3 Marker Method for Burgers' Equation

In this section, we apply the marker method to the solution of the nonlinear Burgers equation. Following the methodology presented in the previous section, the nonlinear

Burgers equation can be written as a nonlinear conservation equation

$$\frac{\partial f}{\partial t} + \frac{\partial}{\partial x} (Vf) = 0 ,$$

where

$$V = \frac{f}{2} - \frac{\mu}{f} \frac{\partial f}{\partial x} . \quad (16)$$

It is interesting to note that the nonlinear term in Burgers' equation appears as a linear term in the convective velocity [first term in Eq.(16)] whereas the linear term in Eq.(2), which accounts for the diffusive process, is represented as a nonlinear term in f [second term in Eq.(16)]. Before presenting numerical results pertaining to the full nonlinear Burgers' equation, we consider the 'wave breaking' effect associated with the quasilinear case [$\mu = 0$ in Eq.(2)]

$$\frac{\partial f}{\partial t} + f \frac{\partial f}{\partial x} = 0 , \quad (17)$$

with initial condition $f(x, 0) = f_0(x)$. The presence of the diffusive term in the original Burgers' equation prevents the solution from becoming multiple valued. The exact solution of Eq.(17) is

$$f(x, t) = f_0(x - ft) . \quad (18)$$

The explicit solution of Eq.(18) for f amounts to a root finding problem. In this paper the bisection method [18] has been used to solve Eq.(18). In the present case, the initial condition was chosen as $f_0(x) = \text{sech}^2 x$. The solution of the quasilinear problem (17) provides a simple theoretical description of a shock wave. The time at which the shock forms may be estimated by identifying it with the earliest time, t_c , at which the profile $f(x, t)$ becomes vertical, that is, the time at which $\partial f / \partial x = \infty$ for some point on the curve. From Eq.(18) we have the general relation

$$\partial f / \partial x = \frac{f'_0}{1 + t f'_0} ,$$

where a prime denotes a differentiation with respect to the argument. For the specific initial profile of $f_0(x) = \text{sech}^2 x$, we have $f'_0(x) = -2\text{sech}^2 x \tanh x$. On using the largest negative value of this expression (namely $x_c = -4\sqrt{3}/9$) to obtain the earliest time, we find $t_c = 1.299$. Fig.6 shows the the initial profile (thick plain line) and the exact solutions at $t = 0.4, 0.8, 1.2$ are shown by thin plain lines. The shape function used is a superGaussian with infinite support. The symbols represents the approximate solutions based on the markers' positions. We note that the marker method is able to capture the transition just before the wave breaking phenomenon very accurately; the algorithm fails around $t \simeq 1.3$ in good agreement with our estimate for the critical time t_c . We would like to point out that the complexity of the algorithm for this *nonlinear* quasilinear problem is the same as that of the *linear* diffusion equation discussed in the previous section. This is in contrast with finite difference methods for which the linear diffusion equation and the nonlinear quasilinear problem (17) would require different algorithms.

Having considered the limit cases of Eq.(2), we now present a numerical example for the full nonlinear Burgers' equation. Given the initial profile of

$$f_0(x) = f(x, 0) = \frac{\mu}{\lambda} (A - 4 \tanh(x/\lambda)) ,$$

where μ , A and λ are constants, the exact solution of Burgers's equation is (see Appendix)

$$f(x, t) = 2\mu \frac{2a e^{\mu t a^2 - ax} + b e^{\mu t b^2 - bx} + c e^{\mu t c^2 - cx}}{2 e^{\mu t a^2 - ax} + e^{\mu t b^2 - bx} + e^{\mu t c^2 - cx}} , \quad (19)$$

where $a = A/2\lambda$, $b = a + 2/\lambda$ and $c = a - 2/\lambda$. Fig.7 shows the exact (thin plain lines) and approximate (symbols) solutions at $t = 0$, $t = 100$ and $t = 200$. The simulation has been carried out with $N = 256$ markers (with an initial uniform spatial distribution) and a time step of integration $\Delta t = 0.1$. Other parameters are: $A = 4.0$, $\lambda = 7.0$ and $\mu = 0.1$. We note that the marker method is able to capture the steepening of the front with a very good accuracy.

4 Marker Method for the Damped Burgers' Equation

In this section, we apply the marker method to the *damped* Burgers' equation

$$\frac{\partial f}{\partial t} + f \frac{\partial f}{\partial x} = -\nu f + \frac{\partial^2 f}{\partial x^2} , \quad (20)$$

where $\nu > 0$ is a constant. This equation has been used in fluid mechanics to model diffusive waves subjected to dissipation [15]. The introduction of a (linear) damping term [first term on the righ-hand side of Eq.(20)] does modify the marker method in a subtle way. For example, consider the simpler equation of

$$\frac{\partial f}{\partial t} = -\nu f , \quad (21)$$

which, given an initial profile $f_0(x) = f(x, 0)$, admits the exact solution of $f(x, t) = e^{-\nu t} f_0(x)$. The marker method can be applied to Eq.(21); the convective velocity is given by

$$V = \frac{\nu}{F} \int_{-\infty}^x F(x', t) dx' . \quad (22)$$

The main difference with the previous examples is that the convective velocity now depends on the approximation solution and its integral. Using the super-Gaussian shape function $S(x) = (3/2 - x^2)e^{-x^2}/\sqrt{\pi}$, the explicit form of the convective velocity reads

$$V(x, t) = \nu \epsilon \frac{\sum_j W_j \psi(z_j)}{\sum_j W_j S(z_j)} \quad (23)$$

where $z_j = z_j(x) = (x - x_j)/\epsilon$ and

$$\psi(x) \equiv \int_{-\infty}^x S(x') dx' = \frac{1}{2} [1 + \text{sgn}(x) \text{erf}(|x|)] + \frac{x}{2} \frac{e^{-x^2}}{\sqrt{\pi}} .$$

Here $\text{sgn}(x)$ is the sign of x . The difficulty with the marker method in this case is due to the behavior of the convective velocity for $x \gg 1$. For example, if the initial profile is a localized Gaussian, $f_0(x) = e^{-x^2}$, the convective velocity, Eq.(22), for large positive x becomes exponentially large, $V \sim e^{x^2}$. In constrast, the convective velocity associated with the diffusion equation ($\partial f/\partial t = \partial^2 f/\partial x^2$), for the same initial profile, increases linearly with

x . Fig.8 shows the approximate and exact solutions of Eq.(21) based on a set of $N = 256$ markers; the initial profile was chosen as $f_0(x) = \text{sech}^2 x$. Although the approximate solution is in excellent agreement with the exact solution for $x < 0$, this is clearly not the case for $x > 1$. The convective velocity for $x > 1$ becomes very large and the tail of $F(x, t)$ for large x becomes 'depleted' of its markers. It is worth noting that the tail of F does not contain useful information since F goes to zero there. The singular behavior for $x \gg 1$ can be alleviated by introducing a threshold in the initial condition

$$f_0(x) = \delta + \text{sech}^2 x ,$$

where $\delta \geq 0$. Subtracting $e^{-\nu t} \delta$ from the numerical solution then yields $F(x, t)$. Fig.9 is the same as Fig.8 except that a non-zero threshold $\delta = 1.0$ has been used. For clarity the factor $e^{-\nu t} \delta$ has not been subtracted from the numerical solution. Clearly the approximate solution is now in excellent agreement with the exact solution.

The convective velocity associated with the damped Burgers's equation, Eq.(20) can be written as

$$V = \frac{F}{2} - \frac{1}{F} \frac{\partial F}{\partial x} + \nu \frac{\int_{-\infty}^x F(x', t) dx'}{F} ,$$

or, in explicit form, as

$$V = \frac{1}{2\epsilon} \sum_j W_j S(z_j) - \frac{1}{\epsilon} \frac{\sum_j W_j S'(z_j)}{\sum_j W_j S(z_j)} + \nu \epsilon \frac{\sum_j W_j \psi(z_j)}{\sum_j W_j S(z_j)} , \quad (24)$$

where $z_j = (x - x_j)/\epsilon$ and a prime denotes a derivative with respect to the argument. There is no known exact solution of the damped Burgers' equation. However accurate approximate solutions to Eq.(20) do exist. For example, Malfliet developed the so-called tanh method [16, 17] to solve certain dispersive equations such as the damped Burgers' equation. He showed that the approximate solution of Eq.(20) can be written as [17]

$$f(x, t) \simeq 2ce^{-\nu t}(1 - \xi) [1 + a_3(t)\xi^3(1 + \xi) + a_5(t)\xi^5(1 + \xi) + a_7(t)\xi^7(1 + \xi) + \dots] , \quad (25)$$

where $\xi = \tanh [c(x - (2c/\nu)(1 - e^{-\nu t}))]$ and

$$\begin{aligned} a_3(t) &= \frac{1}{3} (e^{-\nu t} - 1) , \\ a_5(t) &= -\frac{1}{60c^2} (\nu e^{-\nu t} + 8c^2 e^{-2\nu t} - 40c^2 e^{-\nu t} + 32c^2) . \end{aligned}$$

Here $1/c$ is a constant which plays the role of a characteristic wavelength. Fig.10 shows the approximate solution of the damped Burgers's equation using the marker method (symbols). The plain lines represent the approximate analytical solution given by Eq.(25). The parameters are: $\nu = 0.05$, $c = 1.0$, $\Delta t = 0.01$, $\delta = 1/10$ (threshold) and support parameter $\epsilon = \sqrt{h}$. We note a satisfactory agreement between the numerical and analytical solutions.

An important aspect of the method is its convergence with the number of markers. For the purpose of studying the convergence of the marker method, we define the L^2 norm of the algebraic error as

$$\sigma(t; N) = \left[\delta x \sum_{k=1}^M (f(x_k(t), t) - F_k)^2 \right]^{1/2} , \quad (26)$$

where $x_k(t)$ is the position of the marker at time t , M is the total number of markers that satisfies $X_{\min} < x_k < X_{\max}$ and $\delta x = (X_{\max} - X_{\min})/M$; here X_{\min} and X_{\max} are free parameters. Fig.11 shows the L^2 norm of the error at $t = 0.5$ as a function of the number of markers; other parameters are: $\nu = 0.05$, $c = 1.0$, $\Delta t = 0.01$, $\delta = 1/10$ (threshold), $\epsilon = \sqrt{h}$, $X_{\min} = -X_{\max} = -4.0$. Note that $f(x, t)$ used in Eq.(26), and defined in Eq.(25), is *not* the exact solution. Therefore σ must remain finite as $N \mapsto \infty$. Inspection of Fig.11 shows that about 100 markers are sufficient to obtain a relatively accurate solution for the parameters given above. Note that for N approximately greater than about 100 one cannot infer the convergence of the method since the exact analytical solution is not known. In order to address the convergence of the marker method with an arbitrary number of markers N we return to the linear diffusion equation discussed in Section 2.3. Fig.12 shows the L^2 norm of the algebraic error as a function of the number of markers for the linear diffusion equation at $t = 4$ with a square initial profile [Eq.(14)]. Other parameters are: $\Delta t = 0.01$, $\epsilon = 1/3$, $L = 14.0$, $X_{\min} = -X_{\max} = -6.0$. The number of markers has been varied over 3 orders of magnitude. For intermediate to large values of N the L^2 norm of the error is approximately given by $\sigma = \sigma_0 N^{-0.4}$ (for small values of N the convergence rate is (as can be expected) larger).

5 Conclusions

In this paper we have introduced the marker method for the solution of the damped Burgers' equation. The main idea behind the marker method is to rewrite a given PDE as a conservation equation. A set of markers is then advanced in time (Lagrangian scheme) according to a generalized convective velocity associated with the conservation equation (which itself is an alternative (but exact) form of the original PDE). The information about the approximate solution can be obtained through a convolution of the markers' weights and positions with a shape function. In this paper, we have addressed several aspects of the marker method such as the choice of the shape function and the initial loading of the markers. It has been demonstrated that the marker method yields accurate solutions of the standard Burgers' equation and the damped Burgers' equation. The main advantages of the marker method are its ease of implementation, flexibility and accuracy. Further, the marker method is naturally applicable to PDEs which solutions display one or more shocks since the method is Lagrangian in nature. The marker method is a useful complement to other numerical methods for the solution of PDEs such as the finite difference and the finite element methods.

Acknowledgments

This research was supported by Contract No DE-AC02-76CH03073 and the Scientific Discovery through Advanced Computing (SciDAC) initiative (U.S. Department of Energy).

References

- [1] R.H. Berman, D. Brownrigg and R. Hockney, *Mon. Not. R. Astron. Soc.*, **185**, 861 (1978).
- [2] J. Eastwood, R. Hockney and D. Lawrence, *Comp. Phys. Comm.*, **19**, 215 (1980).
- [3] R.W. Hockney, *Phys. Fluids*, **9**, 1826 (1966).
- [4] R.W. Hockney, R. Warriner and M. Reiser, *Electron Lett.*, **10**, 484 (1974).
- [5] C. Rathmann, J. Vomvoridis and J. Denavit, *J. Comput. Phys.*, **26**, 408 (1978).
- [6] J.M. Dawson, *Rev. Mod. Phys.*, **55**, 403 (1983).
- [7] C.K. Birdsall and A.B. Langdon, *Plasma Physics via Computer Simulations*, McGraw-Hill, New York (1985).
- [8] R.W. Hockney and J.W. Eastwood, *Computer Simulations using Particles*, McGraw-Hill, New York (1981).
- [9] J.L.V. Lewandowski, *Phys. of Plasmas*, **10**, 3204 (2003).
- [10] R. Shanny, J.M. Dawson and J.M. Greene, *Phys. Fluids*, **10**, 1281 (1967).
- [11] J.L.V. Lewandowski, *Can. J. Phys.*, **81**, 1331 (2003).
- [12] J.L.V. Lewandowski, *J. of Scientific Computing*, **21**(2), 174 (2004).
- [13] D.J. Korteweg and G. de Vries, *Philos. Mag.* **39**, 422 (1895).
- [14] J.M. Burgers, *The Nonlinear Diffusion Equation: Asymptotic Solutions and Statistical Problems*, Reidel Press, Boston (1977).
- [15] P.L. Sachdev, *Nonlinear Diffusive Waves*, Cambridge University Press, Cambridge (1987).
- [16] W. Malfliet, *Am. J. Phys.*, **60**, 650 (1992).
- [17] W. Malfliet, *J. Phys. A: Math. Gen.*, **26**, L723 (1993).
- [18] W.S Press, S.A. Teukolsky, W.T. Vetterling and B.P. Flannery, *Numerical Recipes in Fortran*, Cambridge University Press, New York (1992).

Appendix: Analytical Solution of Burgers' Equation

The nonlinear Burgers' equation is

$$\frac{\partial f}{\partial t} + f \frac{\partial f}{\partial x} = \mu \frac{\partial^2 f}{\partial x^2}, \quad (27)$$

where $\mu > 0$ is the diffusion coefficient. It is easy to show that the function

$$\theta(x, t) = \exp\left(-\frac{1}{2\mu} \int f(x, t) dx\right),$$

satisfies the diffusion equation

$$\frac{\partial \theta}{\partial t} = \mu \frac{\partial^2 \theta}{\partial x^2}. \quad (28)$$

Therefore a simple prescription for solving Burgers' equation, Eq.(27), is (given an initial profile $f_0(x) = f(x, 0)$)

- determine $\theta(x, 0) = \exp(-\int f_0(x) dx / 2\mu)$;
- obtain $\theta(x, t)$ by solving the diffusion equation (28); and
- determine $f(x, t)$ from $f(x, t) = -2\mu \partial \theta / \partial x / \theta$.

Consider the following initial profile

$$f_0(x) = f(x, 0) = \frac{\mu}{\lambda} (A - 4 \tanh(x/\lambda)).$$

Using the relation of $\int \tanh x dx = \ln(\cosh x) + C$, we obtain

$$\theta(x, 0) = \widehat{\theta} \exp(-Ax/2\lambda) \cosh^2(x/\lambda), \quad (29)$$

where $\widehat{\theta} = \exp(Ax_0/2\lambda) \operatorname{sech}^2(x_0/\lambda)$ and x_0 are constants. The solution of the diffusion equation, Eq.(28), is

$$\theta(x, t) = \int_{-\infty}^{+\infty} G(\xi, x, t) \theta(\xi, 0) d\xi,$$

where

$$G(\xi, x, t) = \frac{1}{\sqrt{4\pi\mu t}} \exp\left(-\frac{(x-\xi)^2}{4\mu t}\right)$$

is the Green's function. After some algebra one obtains

$$\theta(x, t) = \frac{\widehat{\theta}}{4} \left(2e^{\mu t a^2 - ax} + e^{\mu t b^2 - bx} + e^{\mu t c^2 - cx} \right),$$

where $a = A/2\lambda$, $b = a + 2/\lambda$ and $c = a - 2/\lambda$ and

$$\begin{aligned} f(x, t) &= -\frac{2\mu}{\theta(x, t)} \frac{\partial \theta}{\partial x} \\ &= 2\mu \frac{2ae^{\mu t a^2 - ax} + be^{\mu t b^2 - bx} + ce^{\mu t c^2 - cx}}{2e^{\mu t a^2 - ax} + e^{\mu t b^2 - bx} + e^{\mu t c^2 - cx}}. \end{aligned} \quad (30)$$

For the special case $A = 0$ (see Eq.(29)), Eq.(30) simplifies to

$$f(x, t) = -\frac{4\mu}{\lambda} \frac{\sinh(2x/\lambda)}{\cosh(2x/\lambda) + e^{-4\mu t/\lambda^2}}.$$

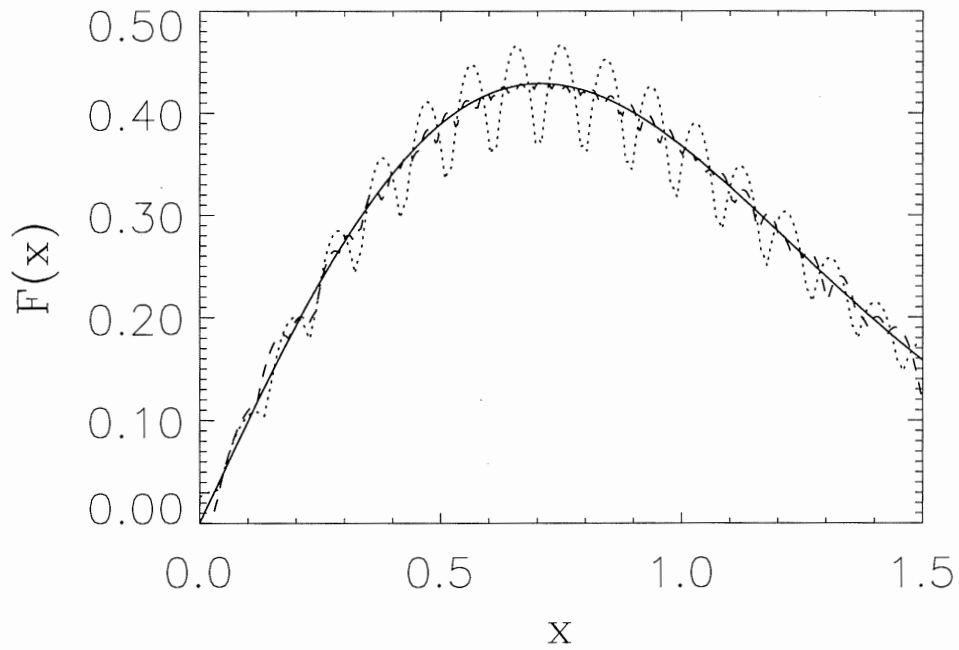


Figure 1: Approximation of the function $f(x) = xe^{-x^2}$ (plain line) based on a set of $N = 32$ markers. The dotted (dashed) line is for the case of uniform (nonuniform) spatial loading. The shape function is a quadratic polynomial [$S(x) = S_3(x)$; see Eq.(11)] with parameter $\epsilon = 0.1$.

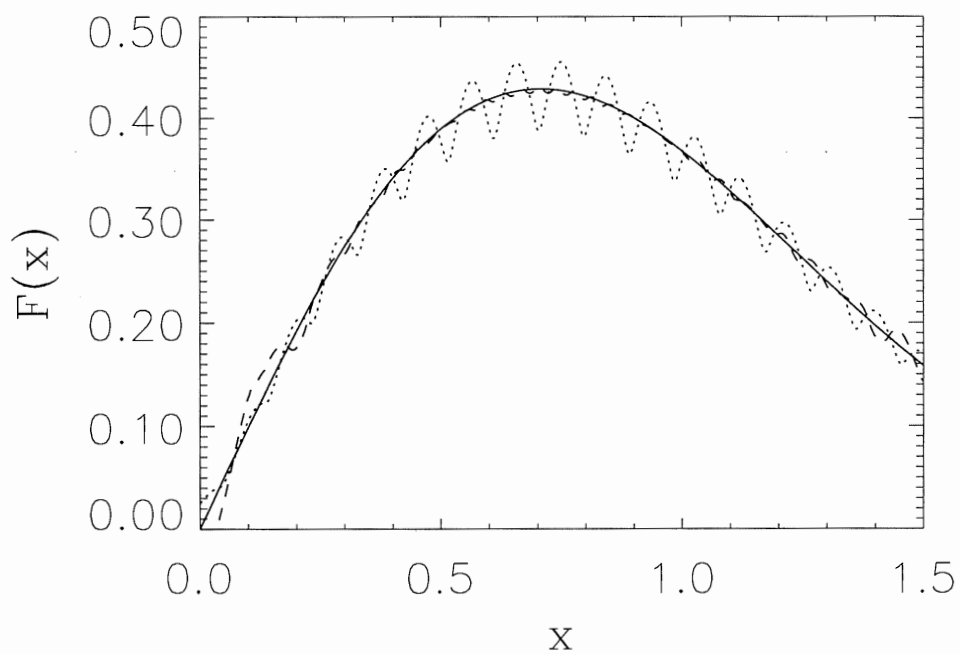


Figure 2: Approximation of the function $f(x) = xe^{-x^2}$ (plain line) based on a set of $N = 32$ markers. The dotted (dashed) line is for the case of uniform (nonuniform) spatial loading. The shape function is a quartic polynomial [$S(x) = S_4(x)$; see Eq.(11)] with parameter $\epsilon = 0.1$.

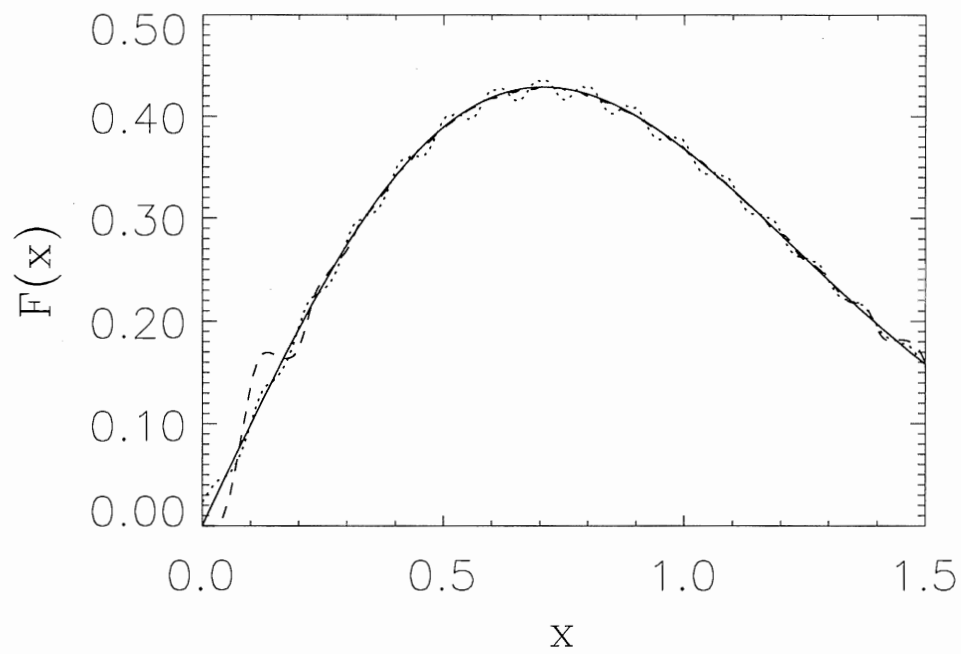


Figure 3: Approximation of the function $f(x) = xe^{-x^2}$ (plain line) based on a set of $N = 32$ markers. The dotted (dashed) line is for the case of uniform (nonuniform) spatial loading. The shape function is based on a quartic polynomial and a Gaussian function [$S(x) = S_6(x)$; see Eq.(11)] with parameter $\epsilon = 0.1$.

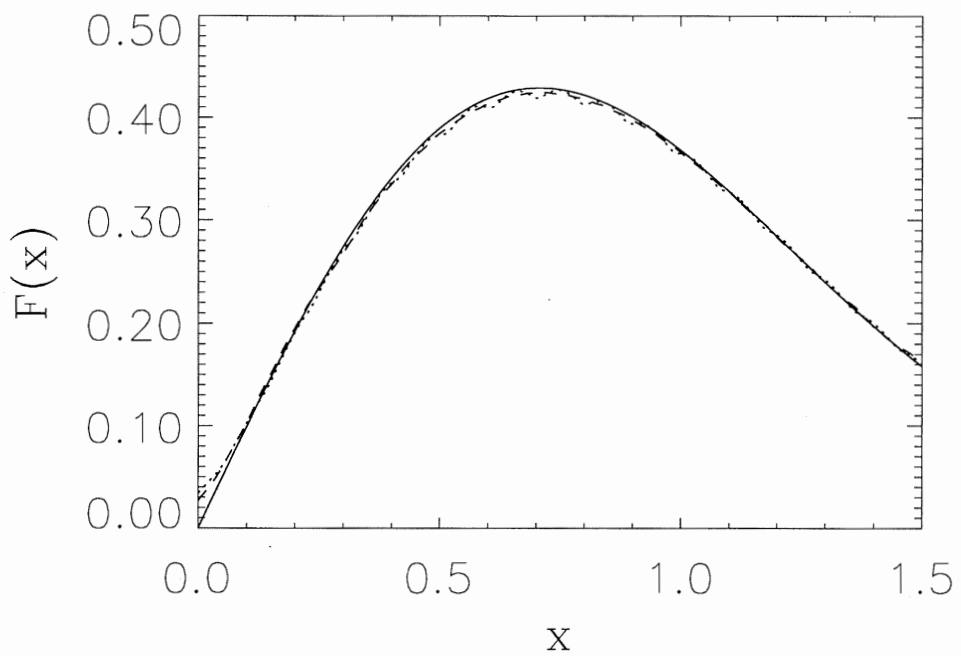


Figure 4: Approximation of the function $f(x) = xe^{-x^2}$ (plain line) based on a set of $N = 32$ markers. The dotted (dashed) line is for the case of uniform (nonuniform) spatial loading. The shape function is a quartic polynomial [$S(x) = S_4(x)$; see Eq.(11)] with parameter $\epsilon = 0.2$.

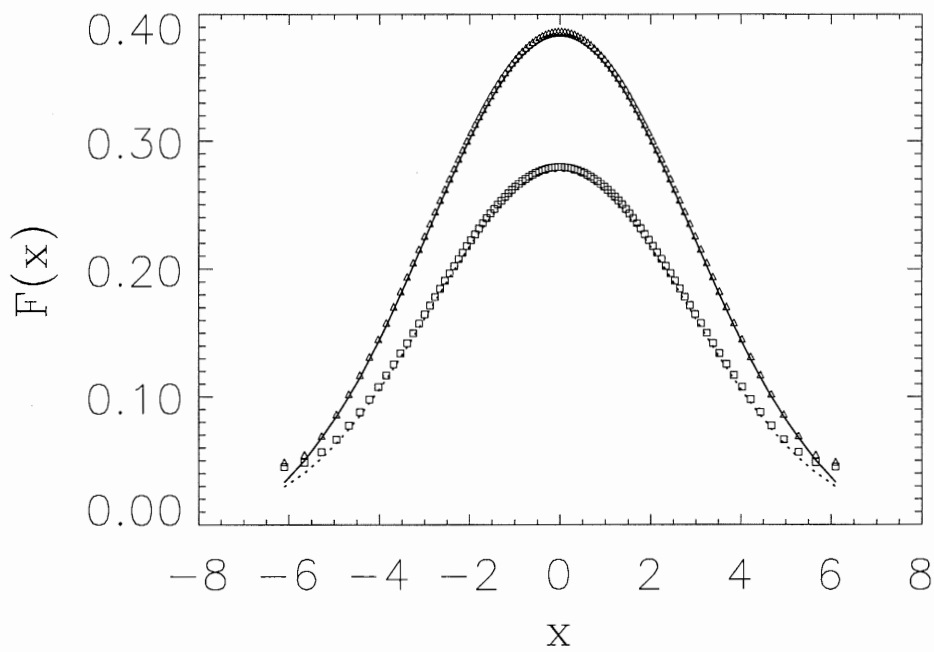


Figure 5: Exact (plain line: $t = 2.0$; dotted line: $t = 4.0$) and approximate (triangles: $t = 2.0$; squares: $t = 4.0$) solutions of the diffusion equation based on a set of $N = 100$ markers. The initial condition is a square profile, Eq.(14). The shape function is a superGaussian [Eq.(15)]. Other parameters are: $\Delta t = 0.01$, $\epsilon = 1/3$ and $L = 14.0$.

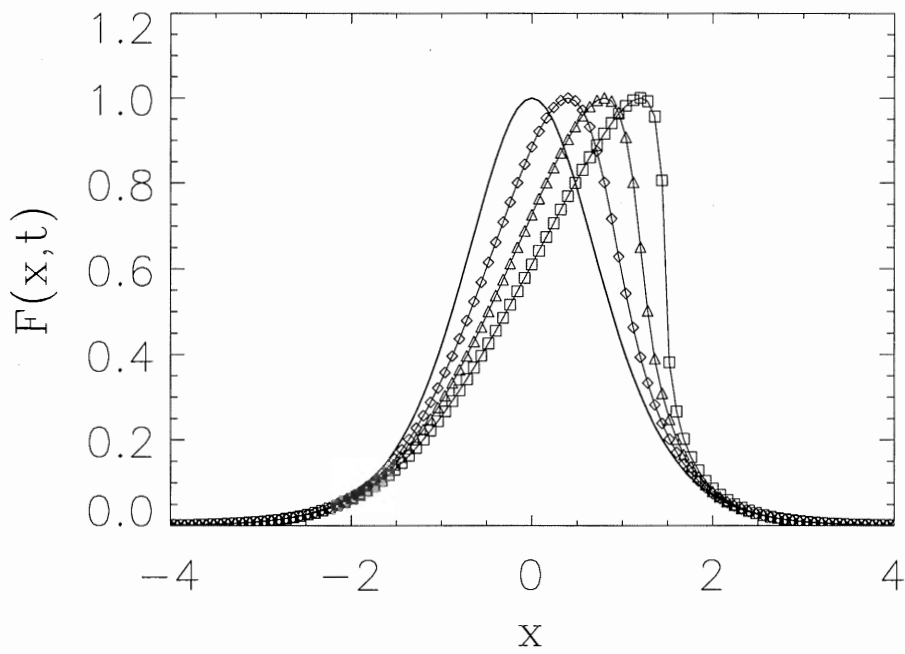


Figure 6: Exact (thin plain lines) and approximate (diamonds: $t = 0.4$, triangles: $t = 0.8$ and squares: $t = 1.2$) solution of the quasilinear equation $\partial f / \partial t + f \partial f / \partial x = 0$ with initial condition $f(x, 0) = \text{sech}^2 x$ (thick plain line). The number of markers is $N = 128$, the time step is $\Delta t = 0.001$ and the support parameter is $\epsilon = \sqrt{h}$.

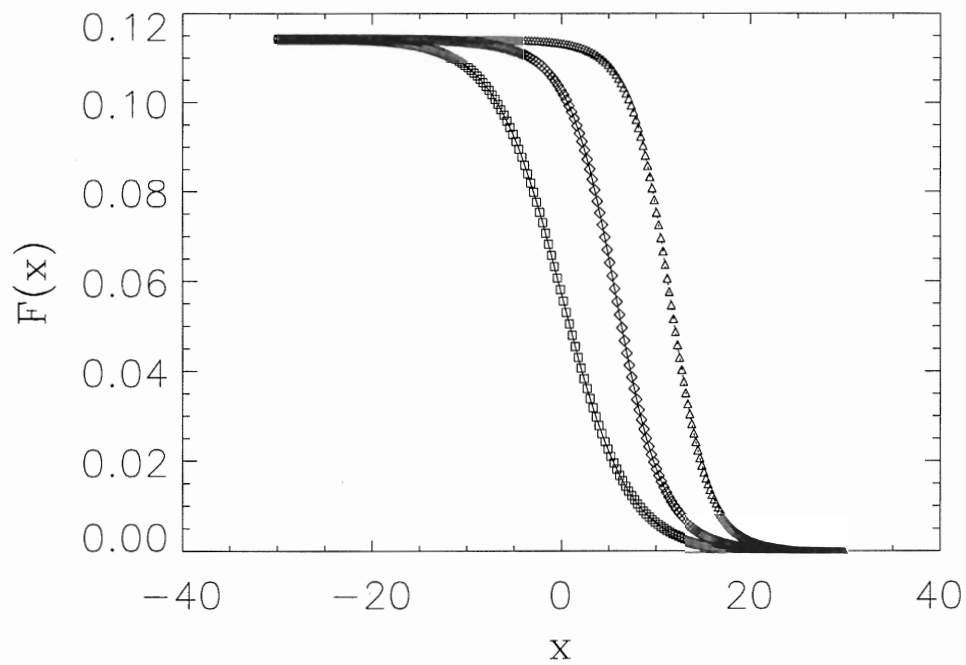


Figure 7: Exact (thin plain lines) and approximate (squares: $t = 0.0$, diamonds: $t = 100$ and triangles: $t = 200$) solution of the nonlinear Burgers equation with initial conditions given by Eq.(19). The parameters are: $\mu = 0.1$, $\lambda = 7.0$ and $A = 4.0$. The number of markers used is $N = 256$ and the time step of integration is $\Delta t = 0.1$.

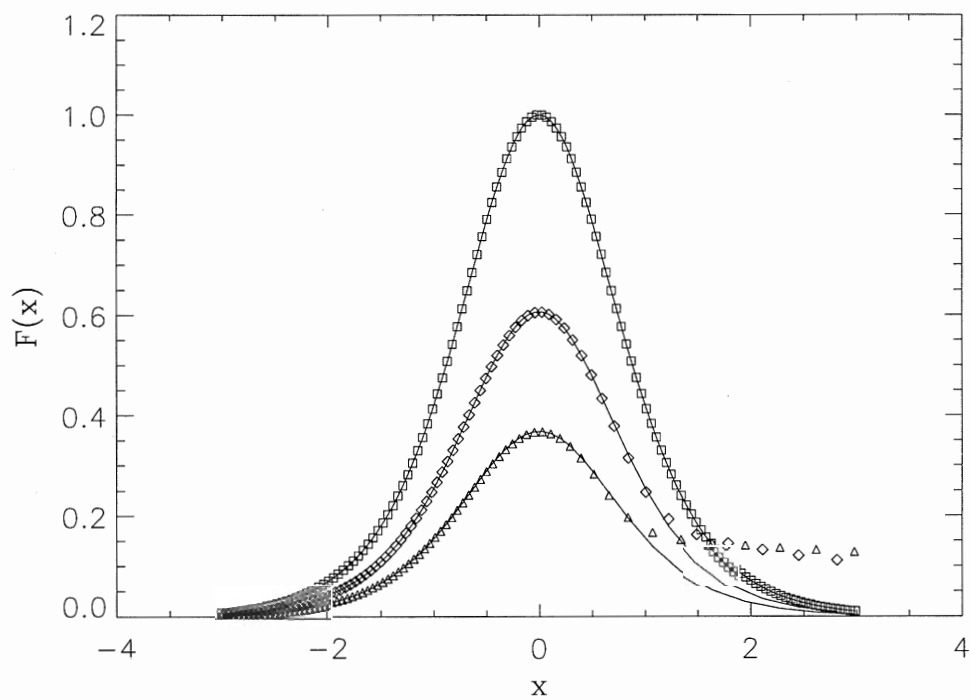


Figure 8: Approximate solution (squares: $t = 0.0$; diamonds: $t = 0.1$; triangles: $t = 0.2$) and exact solution (thin plain lines) of the equation $\partial f/\partial t + \nu \partial f/\partial x = 0$. A set of $N = 256$ markers were uniformly distributed in the interval $x \in [-L, L]$ with $L = 6.0$. The damping parameter is $\nu = 5.0$.

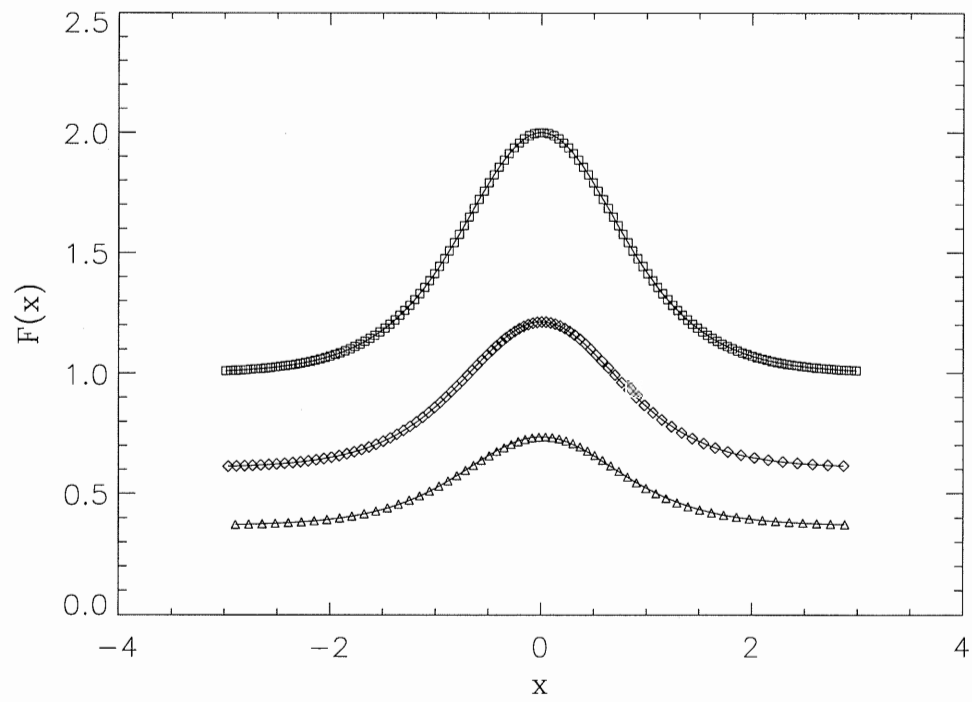


Figure 9: Same as in Fig.8 for a non-zero threshold of $\delta = 1.0$.

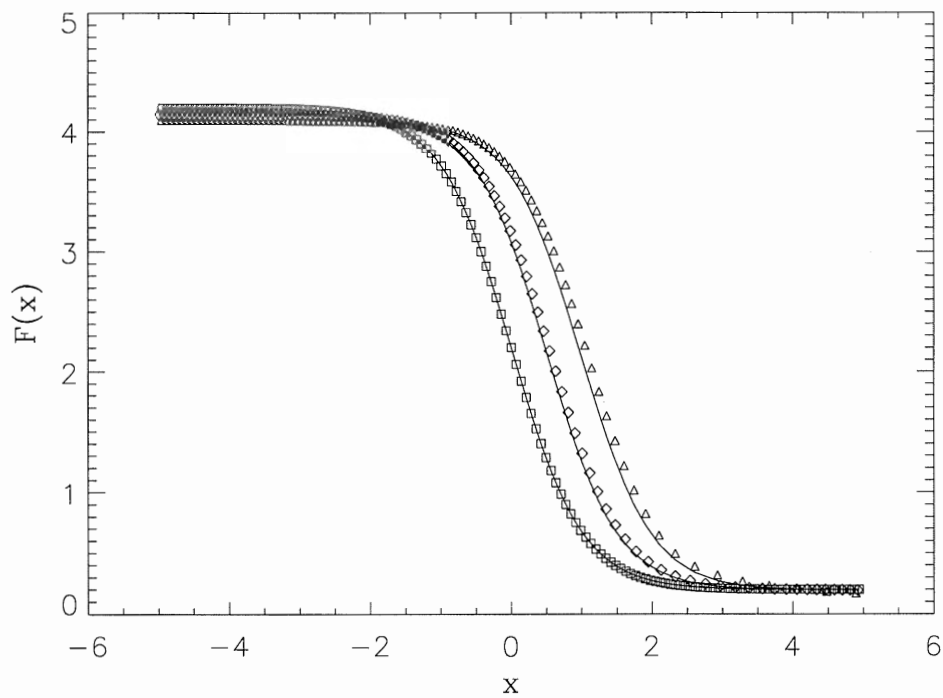


Figure 10: Approximate marker solution (squares: $t = 0.0$; diamonds: $t = 0.25$; triangles: $t = 0.5$) and approximate analytical solution (thin plain lines) of the damped Burgers' equation for a set of $N = 256$ markers. The parameters are: $\nu = 0.05$, $c = 1.0$, $\Delta t = 0.01$ and $\delta = 0.1$.

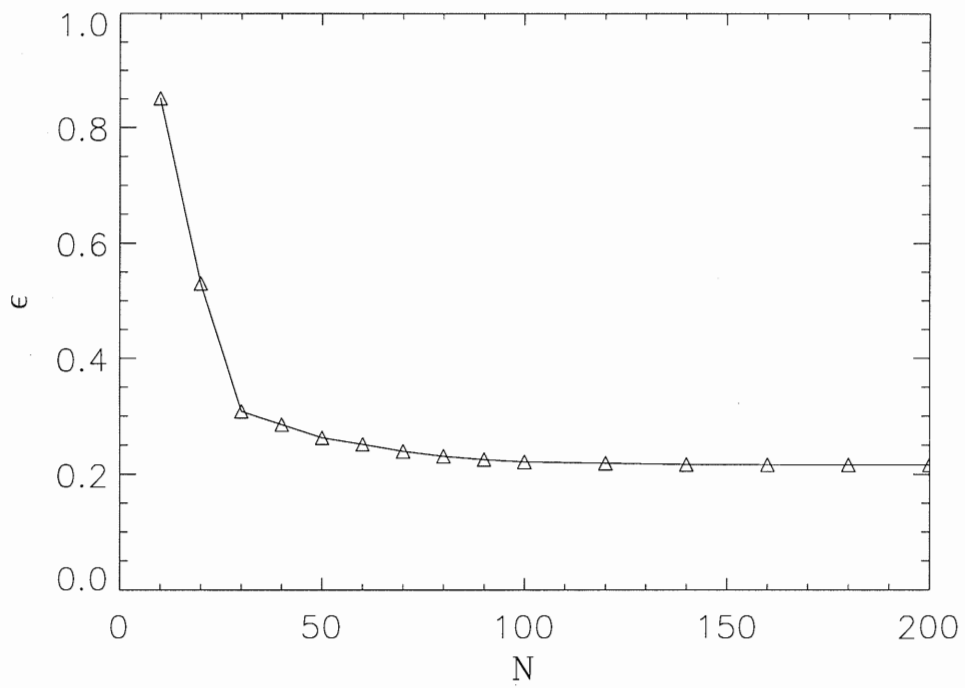


Figure 11: L^2 norm of the error at $t = 0.5$ for the damped Burgers' equation as a function of the number markers. The parameters are: $\nu = 0.05$, $c = 1.0$, $\Delta t = 0.01$ and $\delta = 0.1$.

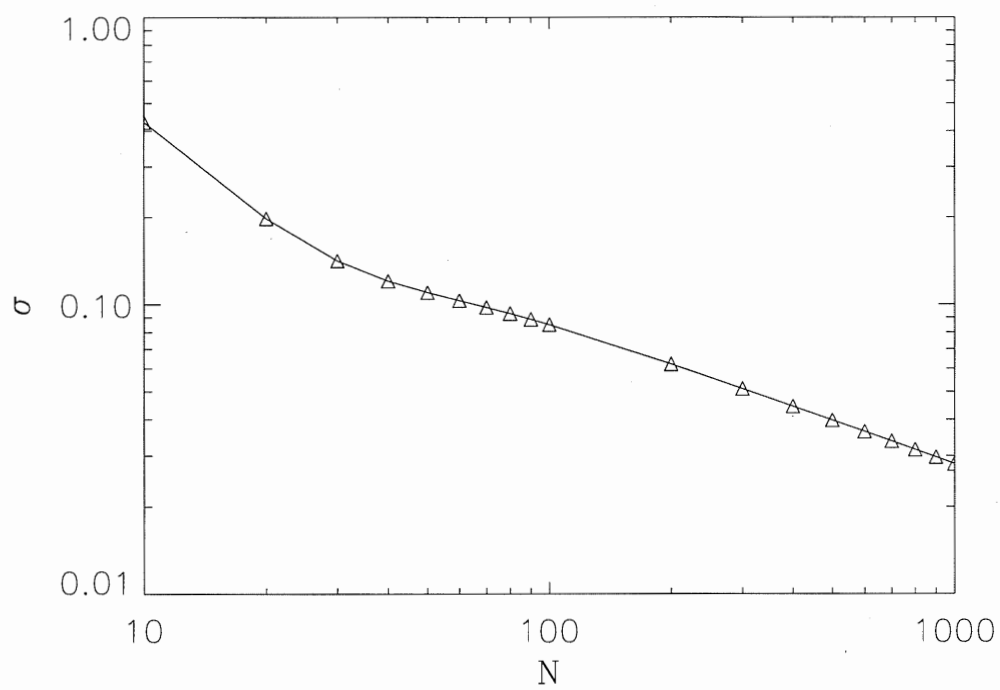


Figure 12: L^2 norm of the error at $t = 4.0$ for the diffusion equation as a function of the number of markers. The initial profile is given by Eq.(14). The parameters are: $\Delta t = 0.01$, $\epsilon = 1/3$, $L = 14$.

External Distribution

Plasma Research Laboratory, Australian National University, Australia
Professor I.R. Jones, Flinders University, Australia
Professor João Canalle, Instituto de Fisica DEQ/IF - UERJ, Brazil
Mr. Gerson O. Ludwig, Instituto Nacional de Pesquisas, Brazil
Dr. P.H. Sakanaka, Instituto Fisica, Brazil
The Librarian, Culham Science Center, England
Mrs. S.A. Hutchinson, JET Library, England
Professor M.N. Bussac, Ecole Polytechnique, France
Librarian, Max-Planck-Institut für Plasmaphysik, Germany
Jolan Moldvai, Reports Library, Hungarian Academy of Sciences, Central Research
Institute for Physics, Hungary
Dr. P. Kaw, Institute for Plasma Research, India
Ms. P.J. Pathak, Librarian, Institute for Plasma Research, India
Dr. Pandji Triadyaksa, Fakultas MIPA Universitas Diponegoro, Indonesia
Professor Sami Cuperman, Plasma Physics Group, Tel Aviv University, Israel
Ms. Clelia De Palo, Associazione EURATOM-ENEA, Italy
Dr. G. Grosso, Istituto di Fisica del Plasma, Italy
Librarian, Naka Fusion Research Establishment, JAERI, Japan
Library, Laboratory for Complex Energy Processes, Institute for Advanced Study,
Kyoto University, Japan
Research Information Center, National Institute for Fusion Science, Japan
Professor Toshitaka Idehara, Director, Research Center for Development of Far-Infrared Region,
Fukui University, Japan
Dr. O. Mitarai, Kyushu Tokai University, Japan
Mr. Adefila Olumide, Ilorin, Kwara State, Nigeria
Dr. Jiangang Li, Institute of Plasma Physics, Chinese Academy of Sciences, People's Republic of China
Professor Yuping Huo, School of Physical Science and Technology, People's Republic of China
Library, Academia Sinica, Institute of Plasma Physics, People's Republic of China
Librarian, Institute of Physics, Chinese Academy of Sciences, People's Republic of China
Dr. S. Mirnov, TRINITI, Troitsk, Russian Federation, Russia
Dr. V.S. Strelkov, Kurchatov Institute, Russian Federation, Russia
Kazi Firoz, UPJS, Kosice, Slovakia
Professor Peter Lukac, Katedra Fyziky Plazmy MFF UK, Mlynska dolina F-2, Komenskeho Univerzita,
SK-842 15 Bratislava, Slovakia
Dr. G.S. Lee, Korea Basic Science Institute, South Korea
Dr. Rasulkhozha S. Sharafiddinov, Theoretical Physics Division, Institute of Nuclear Physics, Uzbekistan
Institute for Plasma Research, University of Maryland, USA
Librarian, Fusion Energy Division, Oak Ridge National Laboratory, USA
Librarian, Institute of Fusion Studies, University of Texas, USA
Librarian, Magnetic Fusion Program, Lawrence Livermore National Laboratory, USA
Library, General Atomics, USA
Plasma Physics Group, Fusion Energy Research Program, University of California at San Diego, USA
Plasma Physics Library, Columbia University, USA
Alkesh Punjabi, Center for Fusion Research and Training, Hampton University, USA
Dr. W.M. Stacey, Fusion Research Center, Georgia Institute of Technology, USA
Director, Research Division, OFES, Washington, D.C. 20585-1290

The Princeton Plasma Physics Laboratory is operated
by Princeton University under contract
with the U.S. Department of Energy.

Information Services
Princeton Plasma Physics Laboratory
P.O. Box 451
Princeton, NJ 08543

Phone: 609-243-2750
Fax: 609-243-2751
e-mail: pppl_info@pppl.gov
Internet Address: <http://www.pppl.gov>